Reticular Synthesis of Multinary Covalent Organic Frameworks

Bing Zhang,[†] Haiyan Mao,[‡] Roc Matheu,[†] Jeffrey A. Reimer,[‡] Sultan A. Alshmimri,[§] Saeed Alshihri,[§] and Omar M. Yaghi*[,†,§]

[†]Department of Chemistry, University of California−Berkeley; Materials Sciences Division, Lawrence Berkeley National Laboratory; Kavli Energy NanoSciences Institute at Berkeley, and Berkeley Global Science Institute, Berkeley, California 94720, United States

[‡]Department of Chemical and Biomolecular Engineering, University of California−Berkeley; Environmental Energy Technologies Division, Lawrence Berkeley National Laboratory, Berkeley, California 94720, United States

[§]UC Berkeley-KACST Joint Center of Excellence for Nanomaterials for Clean Energy Applications, King Abdulaziz City for Science and Technology, Riyadh 11442, Saudi Arabia

S *Supporting Information*

ABSTRACT: Hexagonal hexaminophenyl benzene, tetragonal tetrakis(4-aminophenyl) ethane, and trigonal 1,3,5-tris(p-formylphenyl)benzene were all joined together by imine linkages to yield a 2D porous covalent organic framework with unprecedented **tth** topology, termed COF-346. Unlike the 5 simple existing 2D topologies reported in COFs, COF-346 has 3 kinds of vertices and 2 kinds of edges and is constructed with linkers of 3 kinds of connectivity, and thus represents a higher degree of complexity in COF structures. The success in crystallizing COF-346 was based on precisely chosen geometry and metrics of the linkers and error correction offered by dynamic imine formation. We also report two additional related COFs: a crystalline, porous COF, termed COF-360 with a rare **kgd** topology, as well as the first crystalline, porous COF with defected **tth** topology, termed COF-340.

Reticular chemistry of covalent organic frameworks (COFs) enables the generation of extended structures by design.[1−4] COFs are composed entirely of organic building blocks stitched together through strong covalent bonds. The structures of 2D and 3D COFs are categorized based on their underlying topologies, which can be described based on the number of vertices, edges, rings, and tiles.[3] The vast majority of COFs reported to date have topologies with only one or two kinds of vertices and one kind of edge and are therefore described as edge-transitive.[5] Such nets are the most regular and thus the most likely to form according to one of the principles of reticular chemistry.[6] This, in theory, gives access to a vast number of framework topologies to be targeted in COFs. However, most of these nets are 3D topologies and only 5 kinds of edge-transitive nets with one or two kind of vertices (**hcb**,[2] **hxl**,[7] **kgm**,[8] **sql**[9] and **kgd**[10]) exist for 2D structures (Figure 1a). This constitutes a major limitation in the field of COFs as layered 2D extended structures represent the majority of COF structures. While efforts have been devoted to increasing the structural diversity of 2D COFs, by reticulating more than 2 kinds of linkers,[11−13] or desymmetrizing the pores by changing edge lengths and vertex angles,[14,15] the underlying topologies remain limited to the 5 aforementioned structure
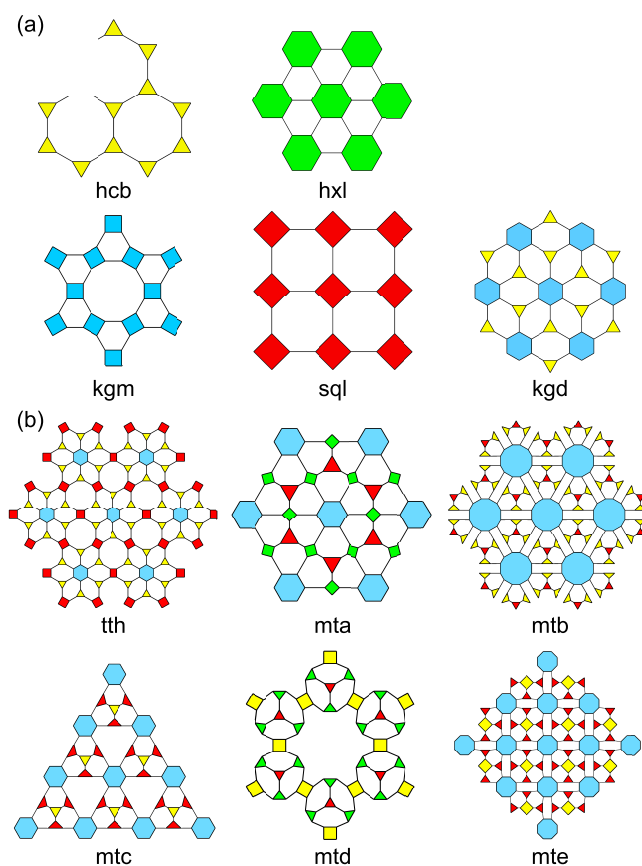

Figure 1. (a) The 5 edge-transitive topologies for 2D COFs. (b) The 6 topologies with 3 kinds of vertices and 2 kinds of edges.

types. To address this challenge, our objective was to target nonedge-transitive nets and synthesize their corresponding COFs by using multiple linkers that will increase the number of vertices and edges and ultimately enhance the structural diversity of 2D COFs. In the Reticular Chemistry Structure Resource (RCSR) database, 6 topologies were identified that have 3 kinds of vertices and two kinds of edges: **tth**, **mta**, **mtb**,

60° + 60° + 120° + 120° = 360°
Angles of linkers match.
Closed ring can form.

60° + 60° + 120° + 90° ≠ 360°
Angles of linkers mismatch.
Closed ring cannot form.

Lengths of linkers match.
Closed ring can form.

Lengths of linkers mismatch.
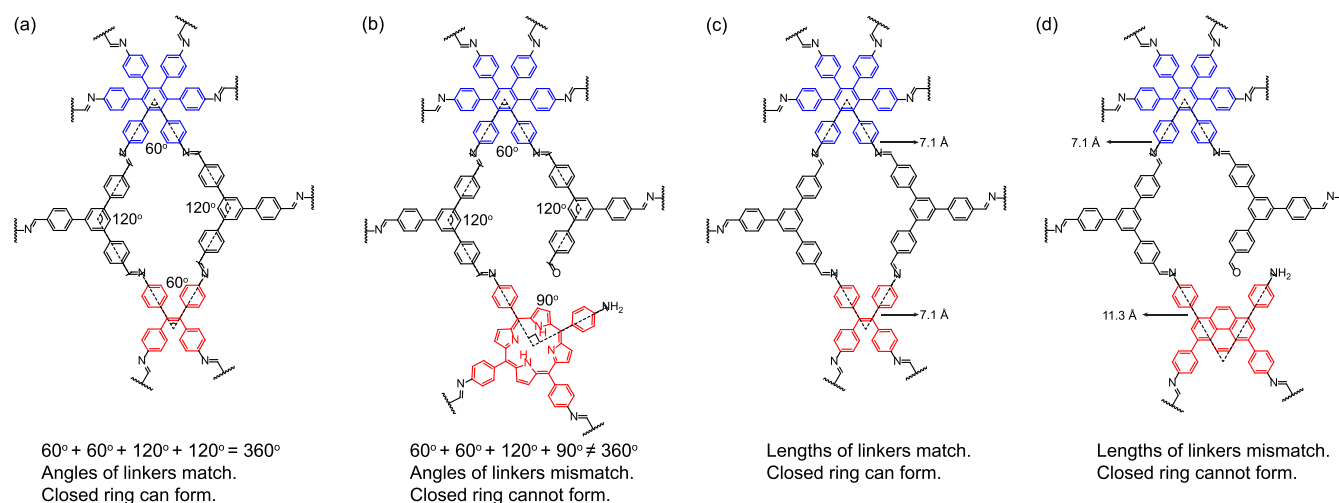Closed ring cannot form.

Figure 2. (a, b) Sum of the angles of linkers are required to be 360° to form a strain-free closed-ring quadrilateral structure. (c, d) Hexatopic and tetratopic linkers are required to have the same length to form a strain-free closed-ring quadrilateral structure.

mtc, **mtd**, and **mte** (Figure 1b).[16] We note that generally, in making COFs with edge-transitive nets, only the angle of the linkers needs to be considered, and isoreticular forms of those COFs can be achieved by increasing the dimensions of the corresponding linkers.[5] However, the challenge in synthesizing COFs with nonedge-transitive topologies is that both the angles and the lengths of the linkers with the corresponding geometries need to be chosen to fit together in a precise manner. This is because the increased number of edges imposes further restriction on the lengths of those edges, which would be suitable to make a COF. In this report, we illustrate using the **tth** topology how directed reticular synthesis can be used to make new multinary COFs, where the linkers employed precisely meet the essential geometry and metric requirements for that net.

To identify the restrictions of angles and lengths imposed by the **tth** net, we deconstructed it into quadrilateral rings, each of which is composed of one hexagon, two triangles, and one quadrilateral (Figures 1b and 2). To form a strain-free, closed quadrilateral, the sum of the angles of the geometric units needs to equal 360°, and the lengths of the hexatopic and tetratopic linkers have to be equal (Figure 2). With these two criteria in mind, we identified hexaminophenyl benzene (HAPB), tetragonal tetrakis(4-aminophenyl) ethane (ETTA), and trigonal 1,3,5-tris(p-formylphenyl)benzene (TFPB) as suitable hexatopic, tetratopic, and tritopic linkers, respectively. The angles of the hexatopic, tetratopic, and tritopic linkers are 60°, 60°, and 120°, respectively. The sum of the angles of one HAPB, one ETTA, and two TFPB is 360° (Figure 2a). Another common tetratopic linker porphyrin tetraamine with a 90° angle cannot be used in this case because the sum of the angles is not 360°, and therefore the closed ring cannot form (Figure 2b). Furthermore, the lengths of HAPB and ETTA (from the points of extension to the intersection) are both 7.1 Å, allowing for closed quadrilaterals to form (Figure 2c). In contrast, if a tetratopic linker 1,3,6,8-tetrakis(4-aminophenyl)-pyrene with a 60° angle is used, even though the sum of the angles satisfies, the mismatched length (11.3 Å) still forbids the closed ring to form (Figure 2d). Similarly, COFs with **mta** and **mtc** topology were designed according to the aforementioned principles, demonstrating the generality of the reticular design of nonedge-transitive COFs (SI, section S11). Lastly, we chose

amine and aldehyde linkers to form imine linkages in the **tth** COF because imine chemistry offers dynamic error correction, which facilitates the crystallization of COFs.[17]

After identifying geometrically equivalent linkers, we screened reaction conditions such as linker ratios and solvent combinations for COF synthesis. A crystalline framework, termed COF-346, was synthesized in a mixture of o-dichlorobenzene and n-butanol with 6 M aqueous acetic acid as the catalyst under solvothermal conditions at 120 °C for 3 d (Figure 3). The product was isolated as a yellow powder, insoluble in common organic solvents such as acetone, tetrahydrofuran, and alcohols. The phase purity of COF-346 was confirmed by scanning electron microscopy (SI, figure S28). Elemental analysis was in good agreement with the calculated formula of $[(HAPB)_1(TFPB)_6(ETTA)_3]_{imine}\cdot(H_2O)_{13}$ for COF-346 (SI, section S2).

The formation of imine linkage in COF-346 was confirmed by Fourier transform infrared (FT-IR) spectroscopy (SI, section S3). The diminished C=O stretching vibration at 1681 cm^{-1} of the aldehydes and the appearance of characteristic C=N stretching vibrations at 1621 and 1202 cm^{-1} corroborated the formation of imine bonds. ^{13}C cross-polarization magic angle spinning nuclear magnetic resonance (MAS NMR) spectroscopy further validated the formation of imine linkages in the COF-346 (SI, section S4). The ^{13}C CP-MAS NMR spectra of COF-346 showed resonance signals at 157.5 ppm, characteristic of the C=N carbons. The remaining signals from 114.9 to 151.1 ppm can be assigned to the aromatic carbons based on liquid spectra of the linker molecules. Digested ^{1}H NMR spectra of the washed and activated COF-346 indicated the presence of all three linkers with a ratio of 1.0:6.2:3.3 (HAPB:TFPB:ETTA), which matches well with the theoretical ratio of 1.0:6.0:3.0 (SI, section S4).

The crystallinity of COF-346 was confirmed by powder X-ray diffraction (PXRD). The powder pattern of this COF displays 6 distinct diffraction peaks at 2.19°, 3.83°, 4.43°, 5.89°, 6.74°, 7.78°, corresponding to the (100), (110), (200), (210), (300), and (220) reflection planes. Pawley refinement was performed on the obtained powder pattern against an eclipsed stacking model constructed in space group P6 to afford unit cell parameters a = b = 46.999 Å, c = 5.413 Å, α = β
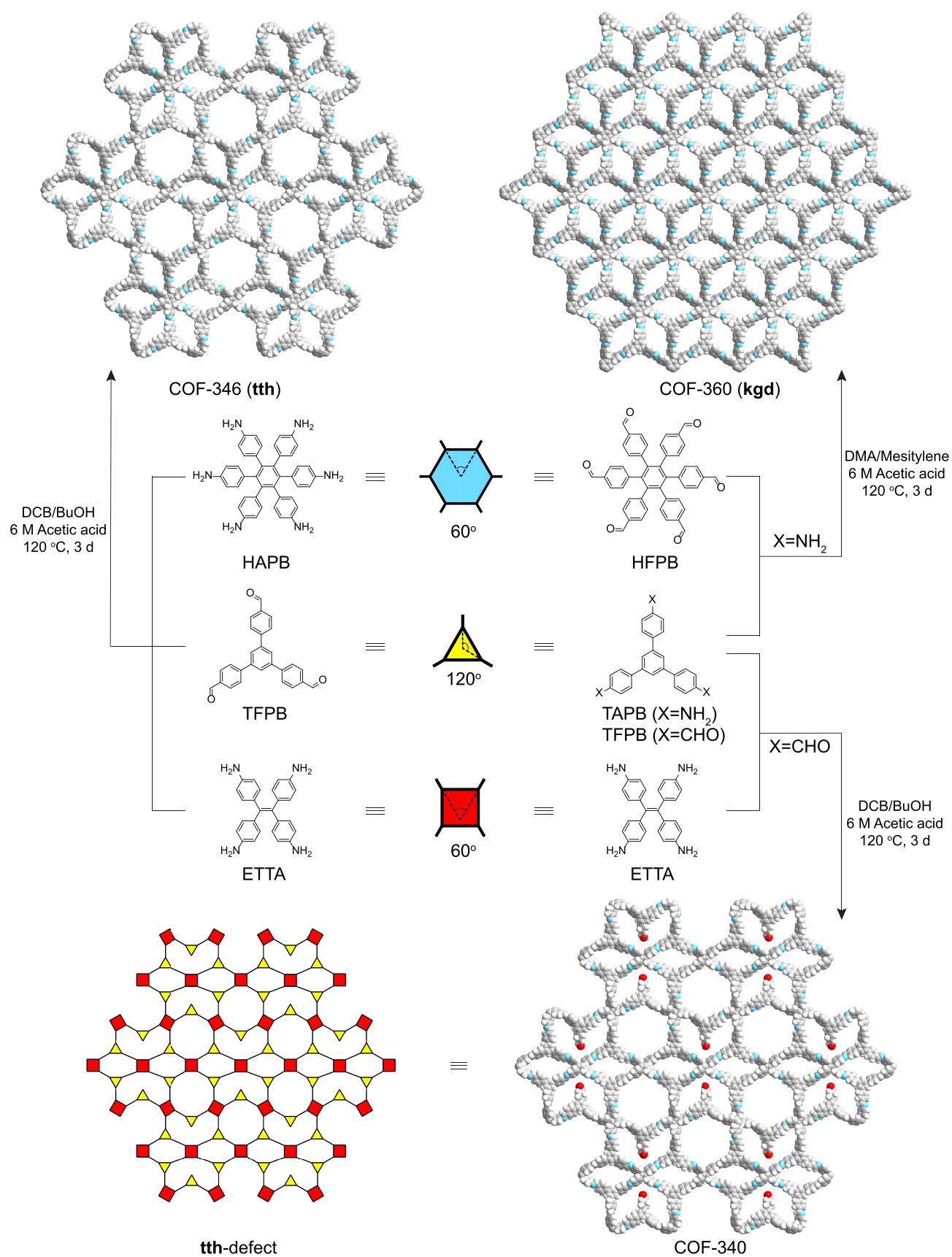
Figure 3. Synthetic scheme for COF-346, -340, and -360. Color code: H, white; C, gray; N; blue; O, red. Frustrated aldehydes are randomly oriented in the COF-340 structure.

= 90°, γ = 120° with good agreement factors (R_{wp} = 8.43% and R_p = 6.23%) (Figure 4a).
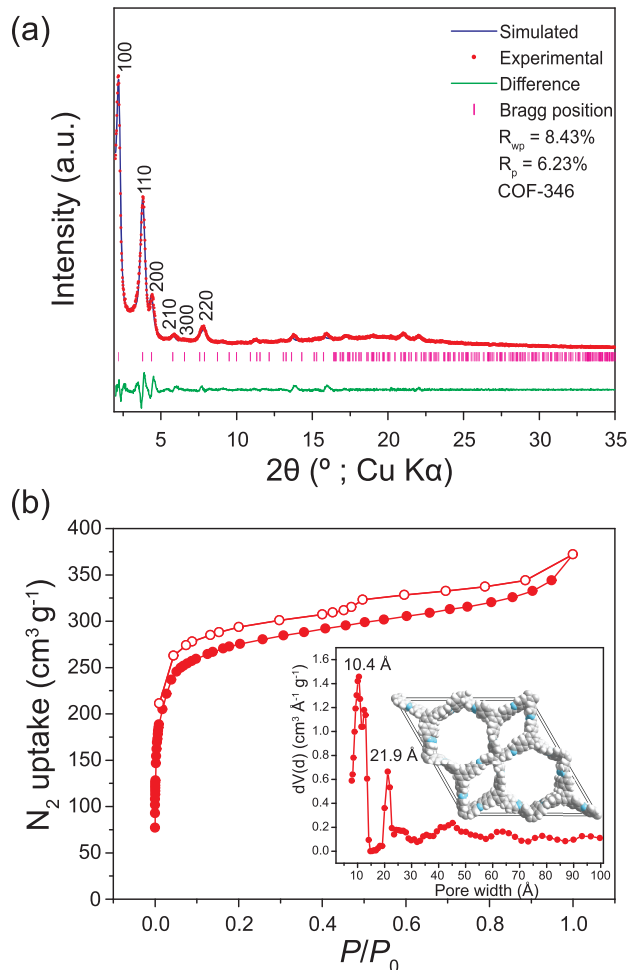

Figure 4. (a) PXRD pattern and Pawley refinement of COF-346. (b) N$_2$ sorption isotherm and pore size distribution diagram of COF-346 using QSDFT method. The hysteresis may be due to a sorbate-induced swelling of the microporous material or restricted filling of the pores.

Permanent porosity of COF-346 was evaluated by N$_2$ adsorption experiments after solvent exchange with tetrahydrofuran and acetone, and activation of the COF *in vacuo* at elevated temperatures. The N$_2$ isotherm was measured at 77 K, and was found to have a characteristic Type I shape, indicating microporosity (Figure 4b). The Brunauer−Emmett−Teller (BET) surface area was calculated to be 1081 m^2 g^{-1}. The pore size distribution of the structure was estimated using a quenched solid density functional theory (QSDFT) model based on slit/cylindrical pore to fit the adsorption branch of the isotherm, as this model gave the lowest fitting error (0.087%). Two kinds of pore widths (10.4 and 21.9 Å) were found for COF-346, in good agreement with the predicted values based on an eclipsed stacking model (11.7 and 22.5 Å).

One of the challenges of synthesizing COFs with multiple components is potential crossover reactions between the linkers. For comparison with the three-component COF-346, we first carried out the reactions between hexatopic HAPB and tritopic TFPB only. However, attempts to synthesize COFs using HAPB and TFPB linkers only yielded poorly crystalline

product, which might be due to the low solubility of HAPB. Therefore, we switched the functionalities and used hexaformylphenyl benzene (HFPB) and tritopic 1,3,5-tris(*p*-aminophenyl)benzene (TAPB) for the synthesis of this model COF (Figure 3). A new 2D COF, termed COF-360, was successfully crystallized as a white powder (SI, section S7). This 3,6 connected net has a rare **kgd** topology. The crystallinity of COF-360 was confirmed by PXRD, and the formation of imine linkages was confirmed by FT-IR and solid-state ^{13}C NMR (SI, section S3, S4, S7).

By comparing the pore sizes of COF-346 and COF-360, the structure of COF-346 was further validated. These two topologies are closely related because the **tth** topology can be converted into the **kgd** topology, by replacing all the tetratopic linkers with hexatopic linkers and adding the corresponding tritopic linkers while retaining the overall metrics of the framework (SI, figure S24). Due to the use of linkers with similar lengths, the sizes of the micropores in COF-346 and COF-360 are expected to match closely. Analysis of the pore size distribution based on the same QSDFT model previously described showed that COF-360 only has one kind of pore of 10.5 Å in diameter, which is close to the micropore of COF-346 (10.4 Å).

It is interesting to note that in the course of our studies we performed the reaction between TFPB and ETTA only and uncovered another crystalline COF, termed COF-340 (Figure 3) (SI, section S7). We were surprised to find that COF-340 has an almost identical PXRD pattern as COF-346 (SI, figure S22). Furthermore, even though a large excess of ETTA was used in the synthesis, free aldehyde groups were still observed by FT-IR (SI, figure S4). Moreover, digestion ^{1}H NMR showed a consistent linker ratio of 3:2 for TFPB and ETTA despite the variation of linker input ratios, suggesting a systematic free aldehyde defect site (SI, figure S13). We speculated that the structure of COF-340 is a defected COF based on the **tth** topology, in which the tetratopic ETTA linkers occupy the hexatopic sites, with frustrated aldehyde groups pointing into the pores due to steric hindrance.[18] This defected COF provides the initial backbone for the crystallization of COF-346 during its synthesis. This was supported by the pore size distribution of COF-340, showing the presence of two kinds of pores (9.3 and 22.0 Å), which are close to the pore sizes of COF-346 (SI, section S7). In contrast, switching the functionalities by using tetrakis(4-formylphenyl) ethene and 1,3,5-tris(*p*-aminophenyl)benzene only yielded amorphous products (SI, figure S17).

In summary, we have designed and synthesized a crystalline, porous COF, termed COF-346, with a new **tth** topology. We also reported COF-340 and COF-360, both of which are structurally related to COF-346. The topological design and reticular synthesis coupled with linkers of precise geometry and metrics allowed us to incorporate linkers with 3 different kinds of connectivity within a 2D COF. This work serves to expand the scope of 2D COF structures and realize new strategies for increasing complexity of COFs by design.

■ ASSOCIATED CONTENT

ⓢ Supporting Information

The Supporting Information is available free of charge on the ACS Publications website at DOI: 10.1021/jacs.9b05626.

Synthetic procedures, FT-IR, NMR, PXRD, porosity analysis, stability data (PDF)

■ AUTHOR INFORMATION

Corresponding Author
*yaghi@berkeley.edu

ORCID ⬤
Bing Zhang: 0000-0001-8350-8624
Roc Matheu: 0000-0001-8601-5219
Jeffrey A. Reimer: 0000-0002-4191-3725
Omar M. Yaghi: 0000-0002-5611-3325

Notes
The authors declare no competing financial interest.

■ REFERENCES

(1) Yaghi, O. M.; Kalmutzki, M. J.; Diercks, C. S. *Introduction to Reticular Chemistry: Metal-Organic Frameworks and Covalent Organic Frameworks*; Wiley-VCH: Weinheim, 2019.

(2) Côte, A. P.; Benin, A. I.; Ockwig, N. W.; O'Keeffe, M.; Matzger, A. J.; Yaghi, O. M. Porous, Crystalline, Covalent Organic Frameworks. *Science* **2005**, *310* (5751), 1166−1170.

(3) El-Kaderi, H. M.; Hunt, J. R.; Mendoza-Cortes, J. L.; Côte, A. P.; Taylor, R. E.; O'Keeffe, M.; Yaghi, O. M. Designed Synthesis of 3D Covalent Organic Frameworks. *Science* **2007**, *316* (5822), 268−272.

(4) Jin, Y.; Hu, Y.; Zhang, W. Tessellated Multiporous Two-dimensional Covalent Organic Frameworks. *Nat. Rev. Chem.* **2017**, *1*, 0056.

(5) Diercks, C. S.; Yaghi, O. M. The Atom, the Molecule, and the Covalent Organic Framework. *Science* **2017**, *355* (6328), No. eaal1585.

(6) Yaghi, O. M.; O'Keeffe, M.; Ockwig, N. W.; Chae, H. K.; Eddaoudi, M.; Kim, J. Reticular Synthesis and the Design of New Materials. *Nature* **2003**, *423*, 705−714.

(7) Dalapati, S.; Addicoat, M.; Jin, S.; Sakurai, T.; Gao, J.; Xu, H.; Irle, S.; Seki, S.; Jiang, D. Rational Design of Crystalline Super-microporous Covalent Organic Frameworks with Triangular Topologies. *Nat. Commun.* **2015**, *6*, 7786.

(8) Zhou, T. Y.; Xu, S. Q.; Wen, Q.; Pang, Z. F.; Zhao, X. One-Step Construction of Two Different Kinds of Pores in a 2D Covalent Organic Framework. *J. Am. Chem. Soc.* **2014**, *136* (45), 15885.

(9) Ding, X.; Guo, J.; Feng, X.; Honsho, Y.; Guo, J.; Seki, S.; Maitarad, P.; Saeki, A.; Nagase, S.; Jiang, D. Synthesis of Metallophthalocyanine Covalent Organic Frameworks That Exhibit High Carrier Mobility and Photoconductivity. *Angew. Chem., Int. Ed.* **2011**, *50* (6), 1289.

(10) Xu, S. Q.; Liang, R. R.; Zhan, T. G.; Qi, Q. Y.; Zhao, X. Construction of 2D Covalent Organic Frameworks by Taking Advantage of the Variable Orientation of Imine Bonds. *Chem. Commun.* **2017**, *53*, 2431.

(11) Chen, X.; Addicoat, M.; Jin, E.; Xu, H.; Hayashi, T.; Xu, F.; Huang, N.; Irle, S.; Jiang, D. Designed Synthesis of Double-stage Two-dimensional Covalent Organic Frameworks. *Sci. Rep.* **2015**, *5*, 14650.

(12) Li, H.; Pan, Q.; Ma, Y.; Guan, X.; Xue, M.; Fang, Q.; Yan, Y.; Valtchev, V.; Qiu, S. Three-Dimensional Covalent Organic Frameworks with Dual Linkages for Bifunctional Cascade Catalysis. *J. Am. Chem. Soc.* **2016**, *138* (44), 14783.

(13) Pang, Z.; Xu, S.; Zhou, T.; Liang, R.; Zhan, T.; Zhao, X. Construction of Covalent Organic Frameworks Bearing Three Different Kinds of Pores through the Heterostructural Mixed Linker Strategy. *J. Am. Chem. Soc.* **2016**, *138* (14), 4710−4713.

(14) Zhu, Y.; Wan, S.; Jin, Y.; Zhang, W. Desymmetrized Vertex Design for the Synthesis of Covalent Organic Frameworks with Periodically Heterogeneous Pore Structures. *J. Am. Chem. Soc.* **2015**, *137* (43), 13772−13775.

(15) Cai, S.; Zhang, K.; Tan, J.; Wang, S.; Zheng, S.; Fan, J.; Yu, Y.; Zhang, W.; Liu, Y. Rationally Designed 2D Covalent Organic Framework with a Brick-Wall Topology. *ACS Macro Lett.* **2016**, *5* (12), 1348−1352.

(16) O'Keeffe, M.; Peskov, M. A.; Ramsden, S. J.; Yaghi, O. M. The Reticular Chemistry Structure Resource (RCSR) Database of, and Symbols for, Crystal Nets. *Acc. Chem. Res.* **2008**, *41*, 1782−1789.

(17) Waller, P. J.; Gándara, F.; Yaghi, O. M. Chemistry of Covalent Organic Frameworks. *Acc. Chem. Res.* **2015**, *48*, 3053−3063.

(18) Gao, Q.; Li, X.; Ning, G.-H.; Xu, H.-S.; Liu, C.; Tian, B.; Tang, W.; Loh, K. P. Covalent Organic Framework with Frustrated Bonding Network for Enhanced Carbon Dioxide Storage. *Chem. Mater.* **2018**, *30* (5), 1762.